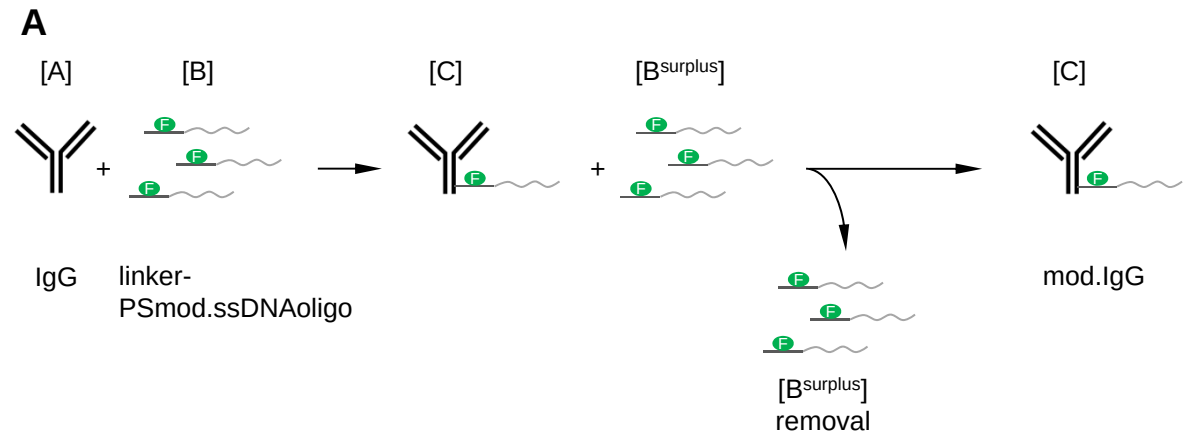
A
[A]
[B]
[C]
[B^surplus]
[C]
IgG
linker-
PSmod.ssDNAoligo
[B^surplus]
removal
mod.IgG

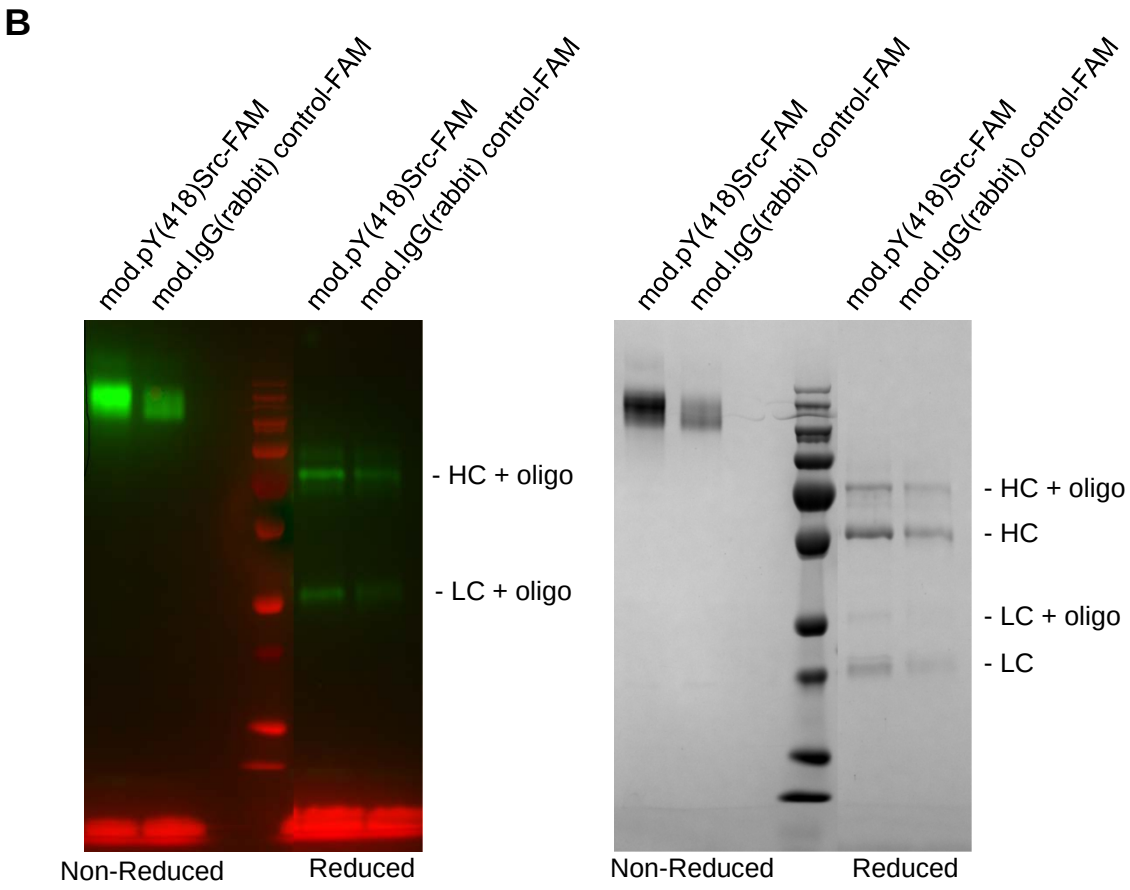
B
mod.pY(418)Src-FAM
mod.IgG(rabbit) control-FAM
mod.pY(418)Src-FAM
mod.IgG(rabbit) control-FAM
mod.pY(418)Src-FAM
mod.IgG(rabbit) control-FAM
mod.pY(418)Src-FAM
mod.IgG(rabbit) control-FAM
- HC + oligo
- LC + oligo
- HC + oligo
- HC
- LC + oligo
- LC
Non-Reduced
Reduced
Non-Reduced
Reduced

C

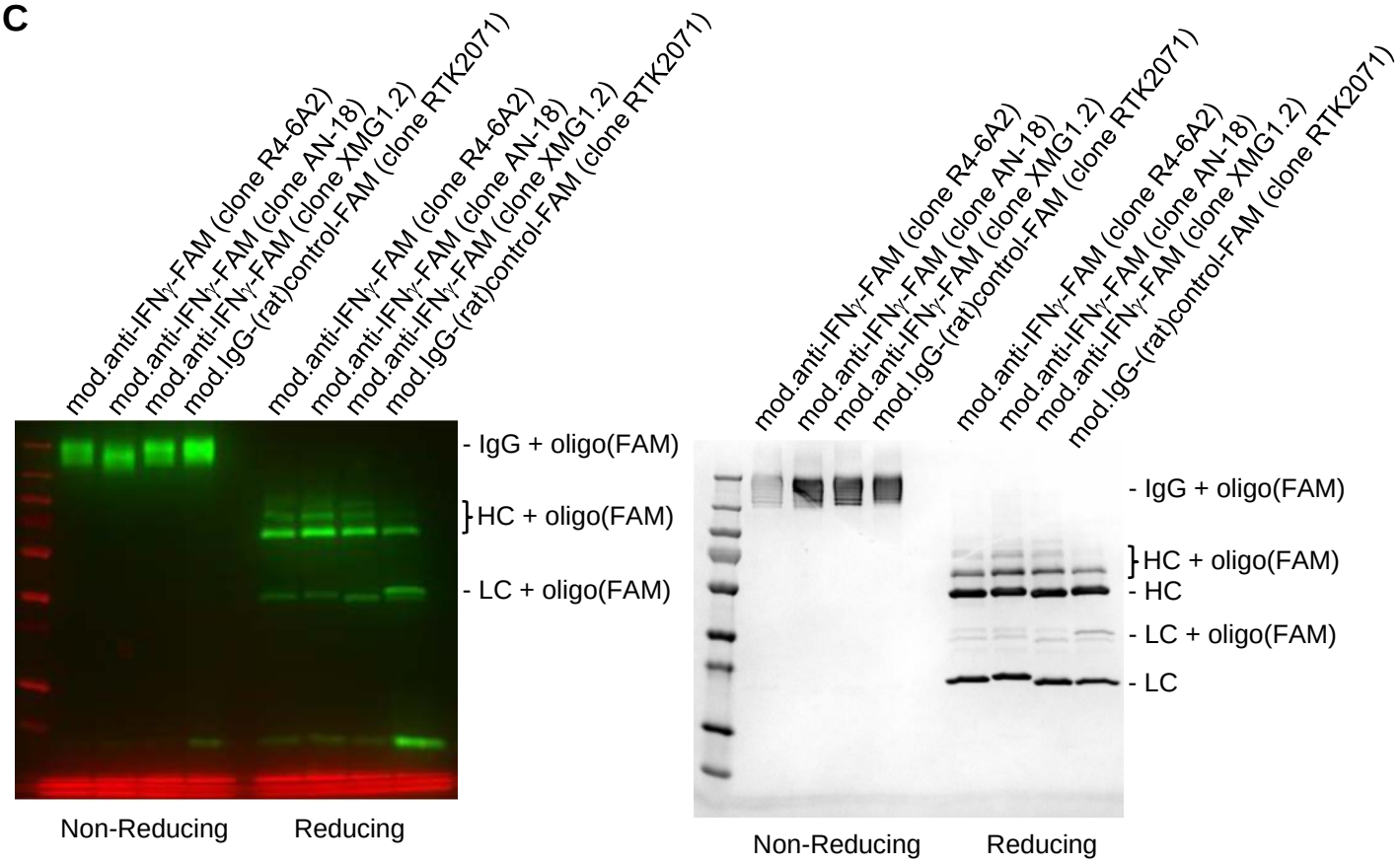

D

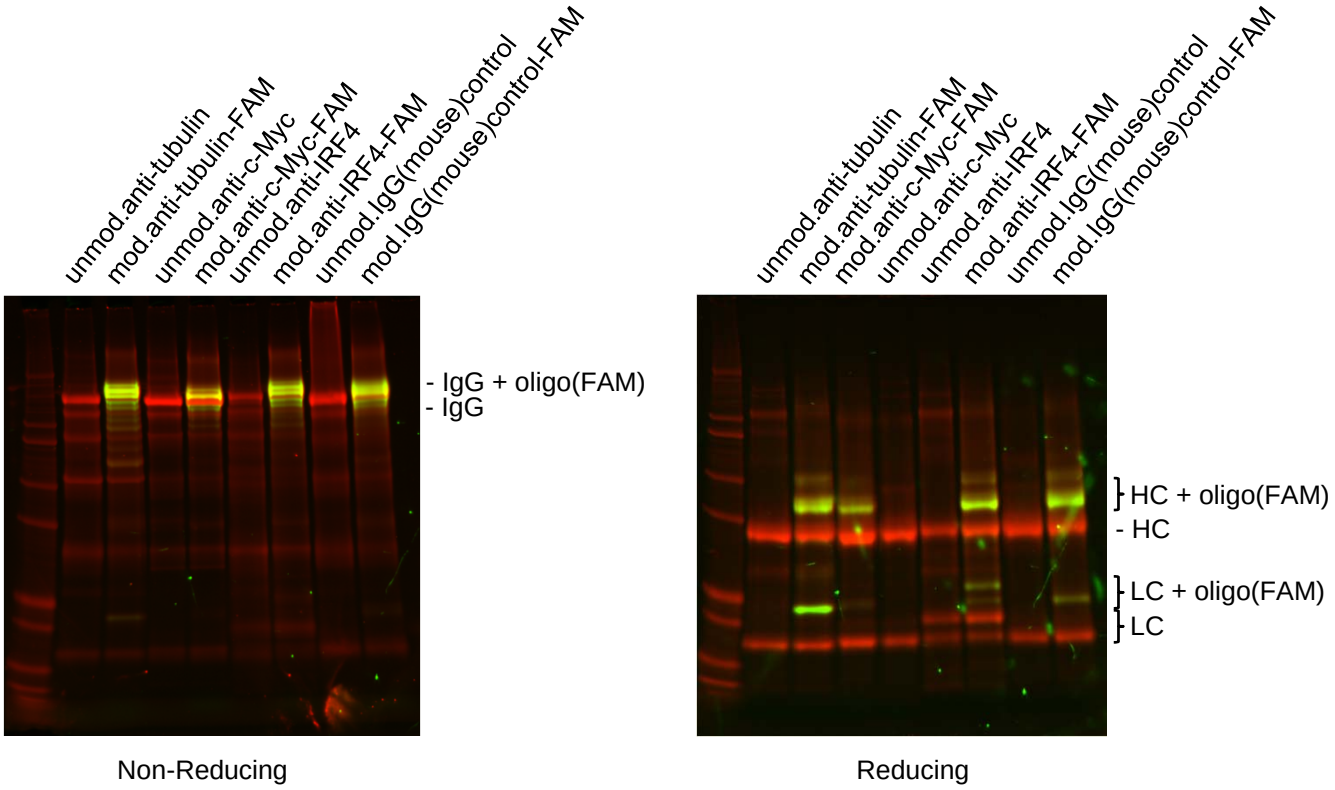

Herrmann, A. *et al.*, Suppl. Fig. 1 cont'd

Supplemental Figure 1: Antibody modification. (**A**) Schematic representation of antibody modification by phosphorothioated (PS) ssDNA-oligo including a linker, optionally carrying a fluorophore (FAM). PS-DNA-oligos were attached to antibodies at the 5' end; 2 C3-propyl-linkers flank the fluorophore. A DBCO-TEG extension of the C3-propyl linker serves conjugation in click-chemistry protocol. (**B-D**) Quality control analyses of modified antibodies by gel-electrophoresis on SDS-PAGE under non-reducing and reducing conditions visualized by fluorophore (FAM) and protein silver-staining. Modified anti-pY(418)-Src antibody and its rabbit IgG control antibody (**B**), modified anti-IFNγ antibody and its rat IgG control (**C**), and modified anti-tubulin, modified anti-c-Myc and modified anti-IRF4 antibodies and their mouse IgG control (**D**) were analyzed after purification to ensure exclusion of contamination by either (i) unbound linker (fluorophore)-ssDNA or (ii) unmodified antibodies. HC= heavy chain, LC=light chain.

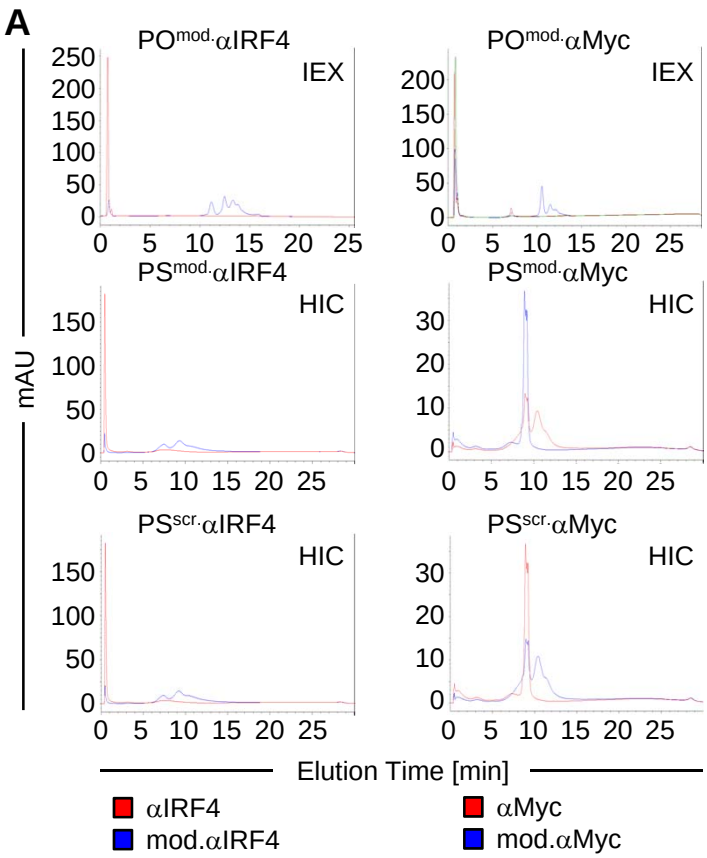

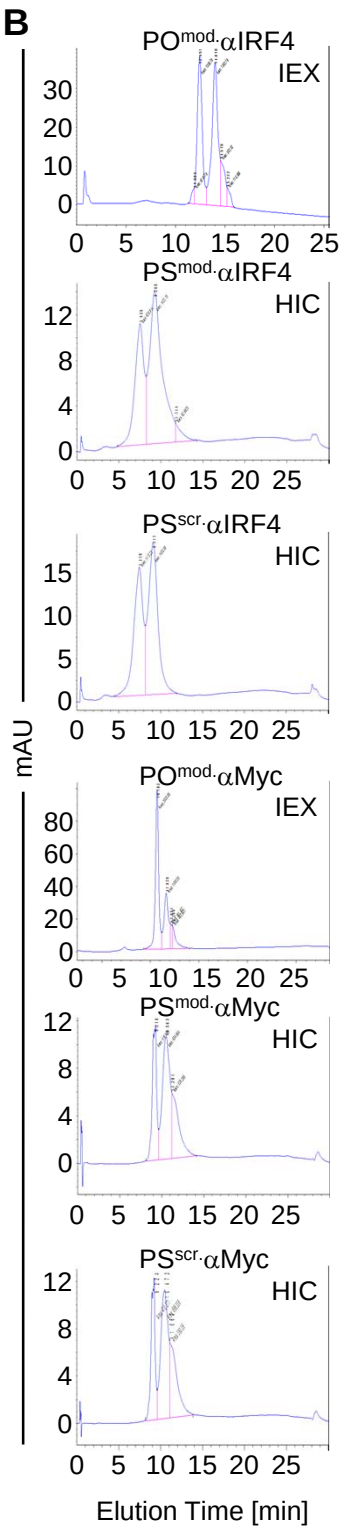

Peak	Elution [min]	Oligo load
1	11.883	1
2	12.451	1
3	14.01	2
4	14.57	3
5	15.222	4

Peak	Elution [min]	Oligo load
1	7.536	1
2	9.268	2
3	11.744	3

Peak	Elution [min]	Oligo load
1	7.47	1
2	9.117	2

Peak	Elution [min]	Oligo load
1	10.702	1
2	11.628	2
3	12.046	3
4	12.269	4

Peak	Elution [min]	Oligo load
1	9.278	0
2	10.563	1
3	11.201	2

Peak	Elution [min]	Oligo load
1	9.224	0
2	10.472	1
3	11.062	2

C

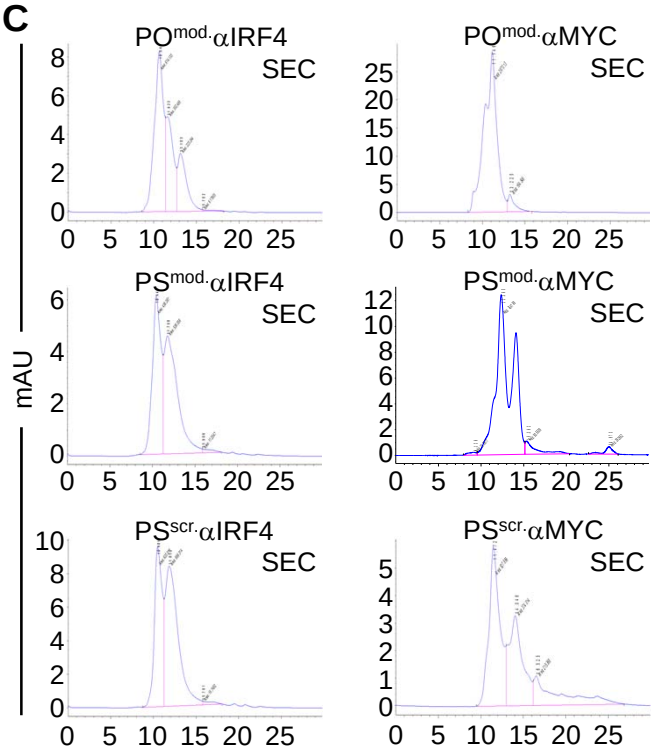

D

Conjugate:	Composition (antibody::DNA-oligo)
PO$^{mod.}$·αIRF4	1-2 ssDNA oligos
PS$^{mod.}$·αIRF4	1-2 ssDNA oligos
PS$^{scr.}$·αIRF4	1-2 ssDNA oligos
PO$^{mod.}$·αMYC	1-2 ssDNA oligos
PS$^{mod.}$·αMYC	1-2 ssDNA oligos
PS$^{scr.}$·αMYC	1-2 ssDNA oligos

E

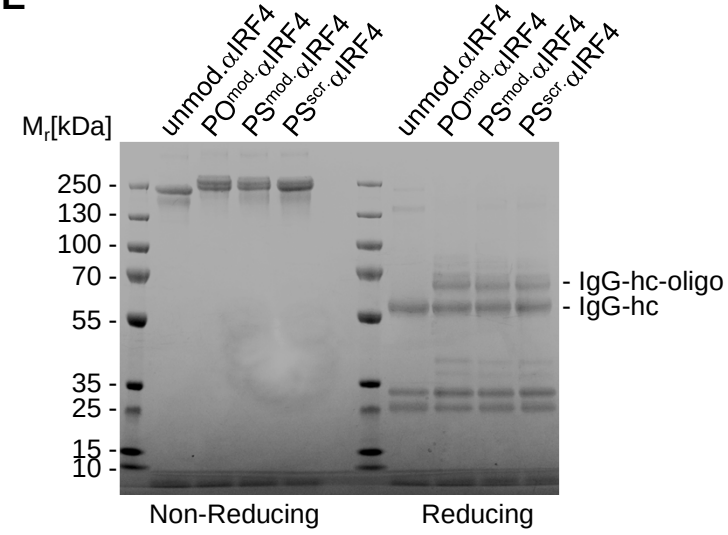

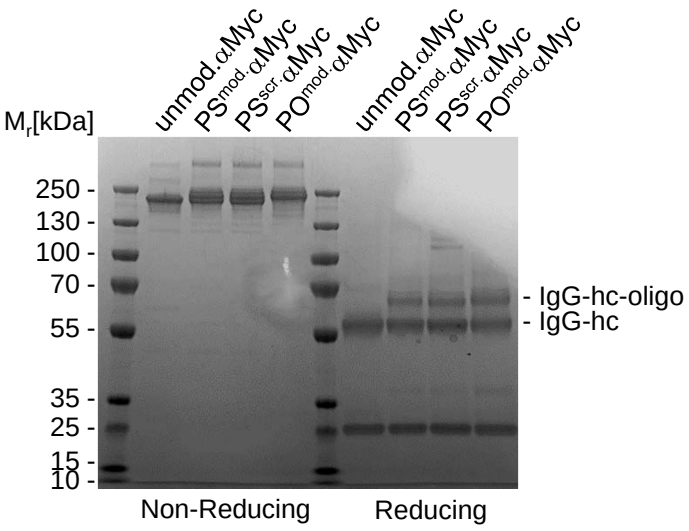

Supplemental Figure 2: Modified antibody quality control. Antibodies against IRF4 and Myc were conjugated with phosphodiester (PO)-ssDNA-oligo, phosphorothioated (PS)-ssDNA-oligo or an alternative phosphorothioated PS-ssDNA-oligo with a scrambled nucleic acid sequence ($PS^{scr.}$). (**A**) Modified antibody populations were separated from unmodified antibodies. (**B**) The modified antibodies were analyzed by ion-exchange (IEX) HPLC or hydrophobic interaction chromatography (HIC), respectively, to determine the number of ssDNA-oligo(s) conjugated per IgG protein (right panels). (**C-D**) Size exclusion chromatography (SEC) HPLC was performed to validate enrichment of homogeneously modified antibody populations conjugated to 1-2 ssDNA oligo(s) per IgG protein upon HPLC purification. (**E**) Additional routine quality control analyses of the modified antibodies (IgG-hc-oligo) were performed by gel-electrophoresis on SDS-PAGE under non-reducing and reducing conditions, followed by protein silver-staining.

A

Gating progress:

All cells	Gated population; new gate on FAM+ cells	Conversion to "zebra plot"	Assessment of FAM+ cells upon treatment

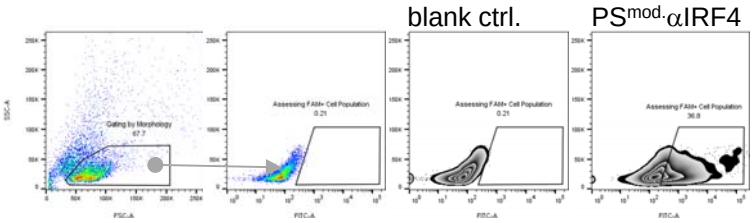

B

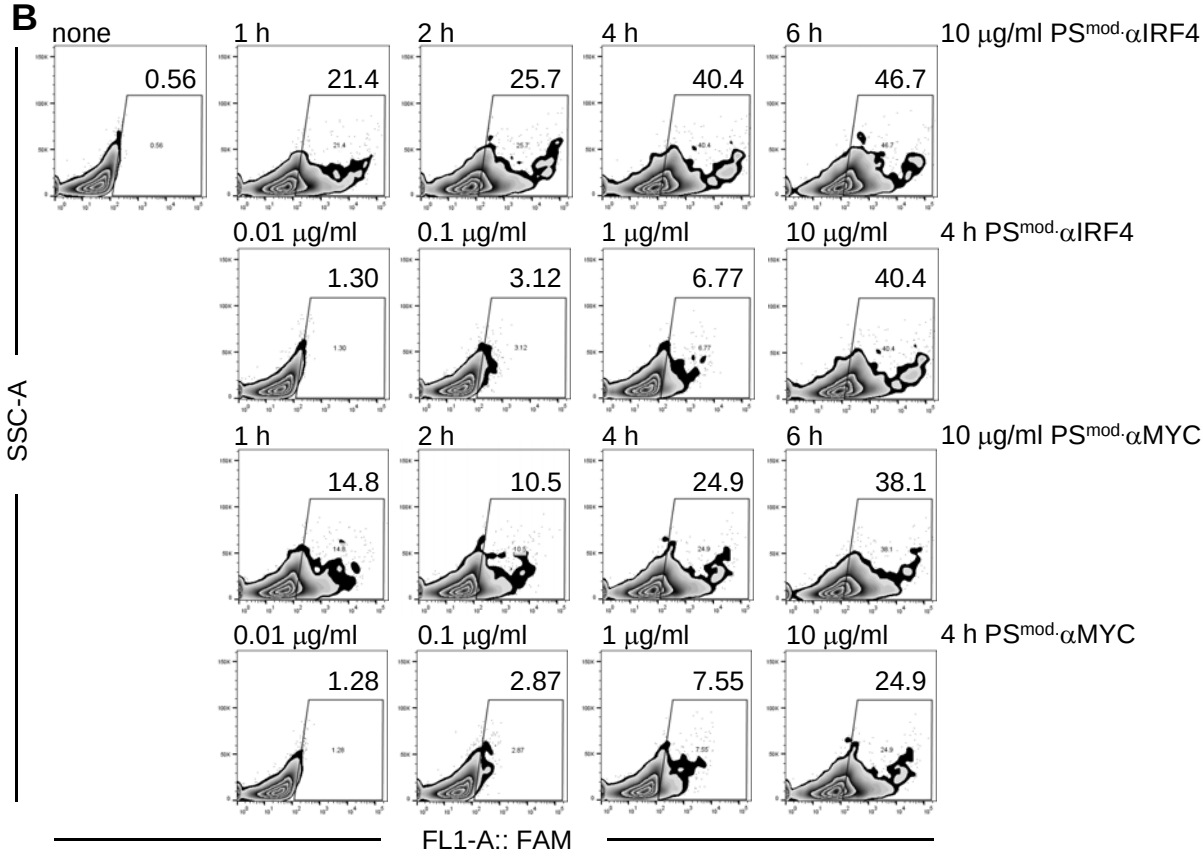

C

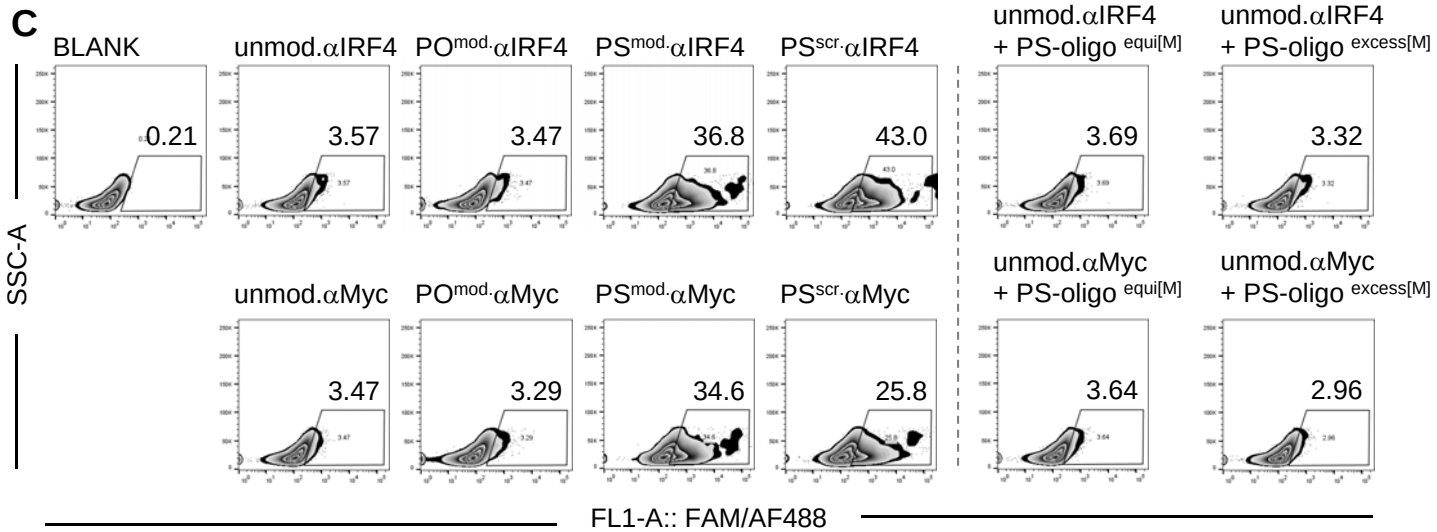

Herrmann, A. *et al.*, Suppl. Fig. 3

D

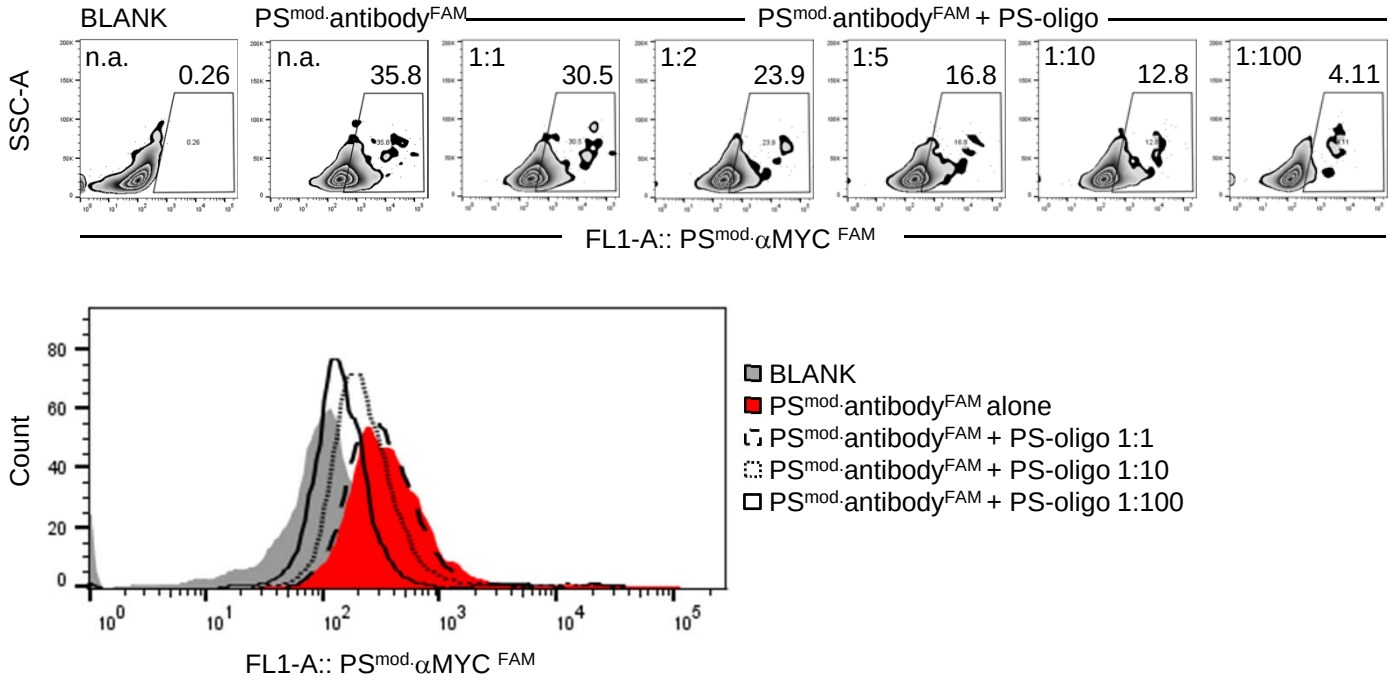
BLANK
PS^mod.antibody^FAM
PS^mod.antibody^FAM + PS-oligo
SSC-A
n.a.
0.26
n.a.
35.8
1:1
30.5
1:2
23.9
1:5
16.8
1:10
12.8
1:100
4.11
FL1-A:: PS^mod.αMYC FAM
Count
BLANK
PS^mod.antibody^FAM alone
PS^mod.antibody^FAM + PS-oligo 1:1
PS^mod.antibody^FAM + PS-oligo 1:10
PS^mod.antibody^FAM + PS-oligo 1:100
FL1-A:: PS^mod.αMYC FAM

E

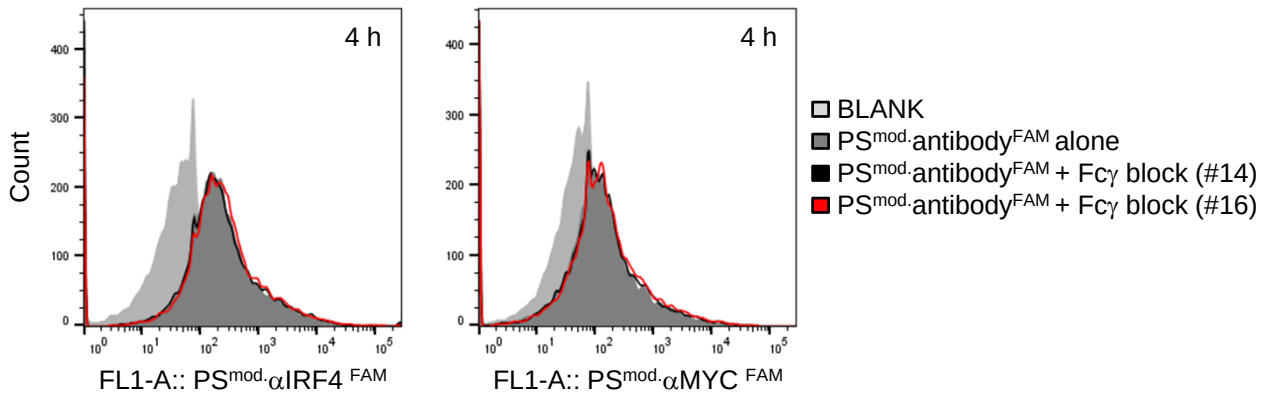
4 h
4 h
Count
BLANK
PS^mod.antibody^FAM alone
PS^mod.antibody^FAM + Fcγ block (#14)
PS^mod.antibody^FAM + Fcγ block (#16)
FL1-A:: PS^mod.αIRF4 FAM
FL1-A:: PS^mod.αMYC FAM

F

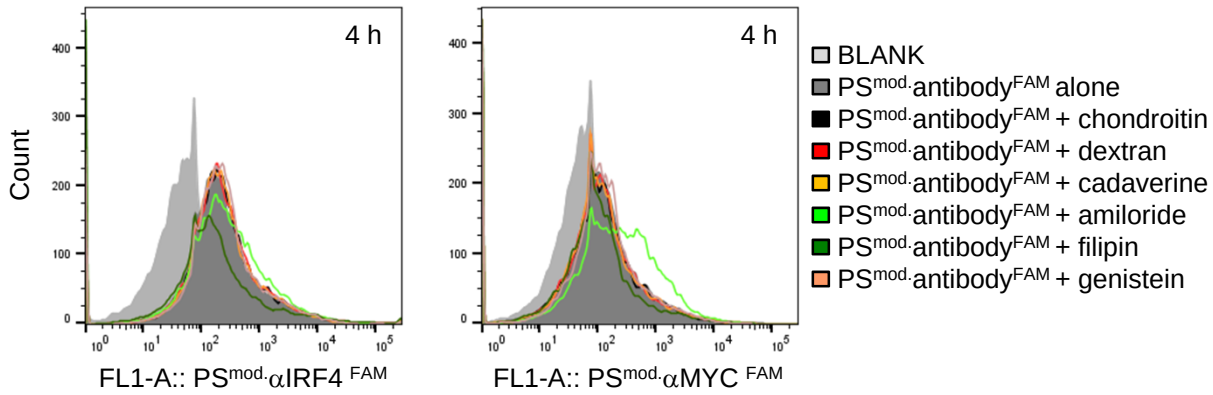
4 h
4 h
Count
BLANK
PS^mod.antibody^FAM alone
PS^mod.antibody^FAM + chondroitin
PS^mod.antibody^FAM + dextran
PS^mod.antibody^FAM + cadaverine
PS^mod.antibody^FAM + amiloride
PS^mod.antibody^FAM + filipin
PS^mod.antibody^FAM + genistein
FL1-A:: PS^mod.αIRF4 FAM
FL1-A:: PS^mod.αMYC FAM

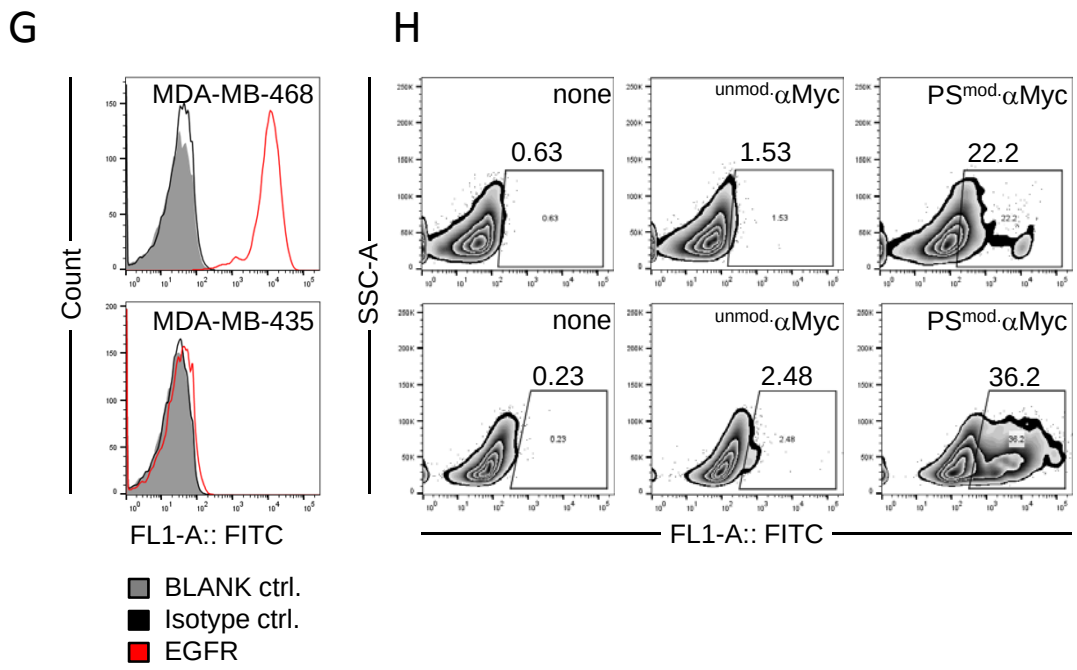
G
H
MDA-MB-468
MDA-MB-435
Count
FL1-A:: FITC
BLANK ctrl.
Isotype ctrl.
EGFR
SSC-A
none
unmod.αMyc
PSmod.αMyc
0.63
1.53
22.2
0.23
2.48
36.2
FL1-A:: FITC

I

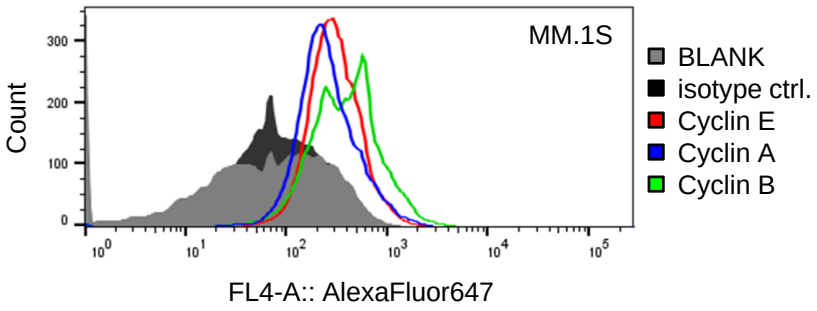
MM.1S
Count
FL4-A:: AlexaFluor647
BLANK
isotype ctrl.
Cyclin E
Cyclin A
Cyclin B

J

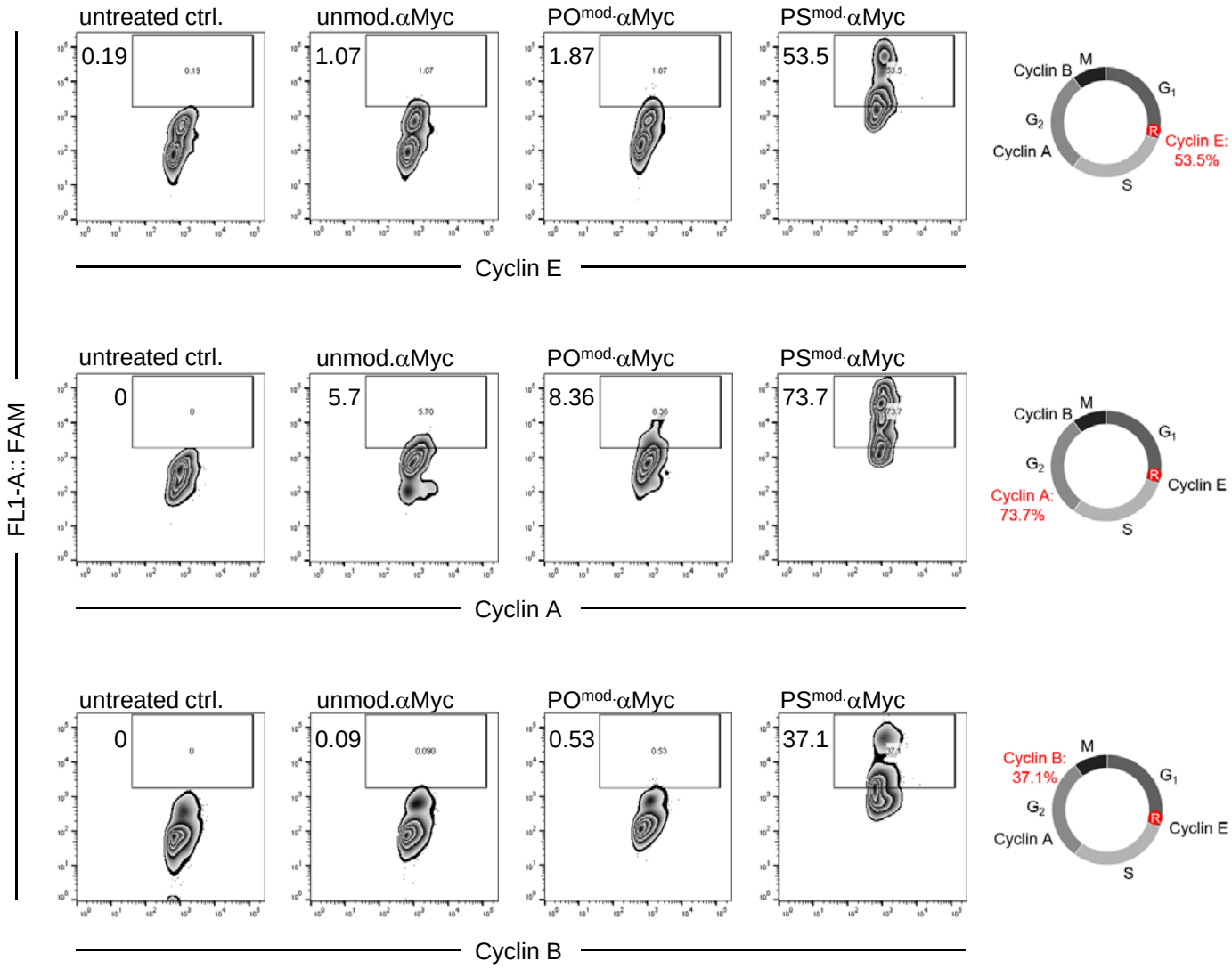
FL1-A:: FAM
untreated ctrl.
unmod.αMyc
PO mod. αMyc
PS mod. αMyc
0.19
1.07
1.87
53.5
Cyclin E
Cyclin B
M
G1
G2
S
R
Cyclin A
Cyclin E: 53.5%
0
5.7
8.36
73.7
Cyclin A
Cyclin A: 73.7%
0.09
0.53
37.1
Cyclin B: 37.1%

Supplemental Figure 3: PS-DNA oligo-modified antibodies undergo cellular internalization. (**A**) Flow cytometric analysis was employed to determine whether covalently linking phosphorothioation of ssDNA-oligos to IgGs (fluorescently labeled) is critical in enabling their cellular entry. Flowchart illustrates gating procedure. (**B**) IRF4 and Myc antibodies were tested for cellular uptake, which is dose and time-dependent. (**C**) Cellular internalization of PS-DNA oligo-modified antibodies is also independent of the PS-DNA oligo nucleic acid sequences and requires physical attachment of the PS oligos to antibodies. IRF4 and Myc antibodies modified by two different PS-DNA oligo nucleic acid sequences (scr, scrambled) were incubated in human multiple myeloma MM.1S cells, followed by flow cytometry analysis. In the same flow cytometric analysis, little to no intra-cellar uptake of the antibodies conjugated with non-phosphorothioated PO-ssDNA-oligo to IgGs or equimolar (stochiometric 1:1 mix; IgG:oligo) and excess molar PS-oligo mixing with IgG's (stochiometric 1:2 mix; IgG:oligo) without conjugation (right panels, columns 5, 6) was observed. Unmodified (unmod.) antibodies were included as non-cell-penetrating control (left panels, column 2). (**D**) Competition assay reveals PS-DNA-oligos impetes PS-modified antibody uptake in human MM.1S multiple myeloma cells in a dose-dependent manner. Cellular internalization was independent of potential engagement to Fcγ receptor (**E**) and endocytic activity of tumor cells (**F**). (**G, H**) Cellular internalization of PS-modified antibodies is independent of EGF receptor expression. Internalization of PS-modified antibody by EGFR-negative human breast cancer cells, MDA-MB-435, was compared to EGFR-positive human breast cancer cells, MDA-MB-468, as assessed by flow cytometry. (**I, J**) Cell-cycle/membrane potential and cellular internalization of PS-modified antibodies. (**I**) Expression of cyclins by an unsynchronized population of human multiple myeloma MM.1S cells assessed by flow cytometry. (**J**) Cyclin E, cyclin A, cyclin B-positive cells, especially cyclin A-positive cells, which are known to have higher polarized/maintained cell membrane potential, show considerably increased cellular internalization of PS-modified antibodies, relative to pooled cells (**A-D**). Data represent 3 independent experiments.

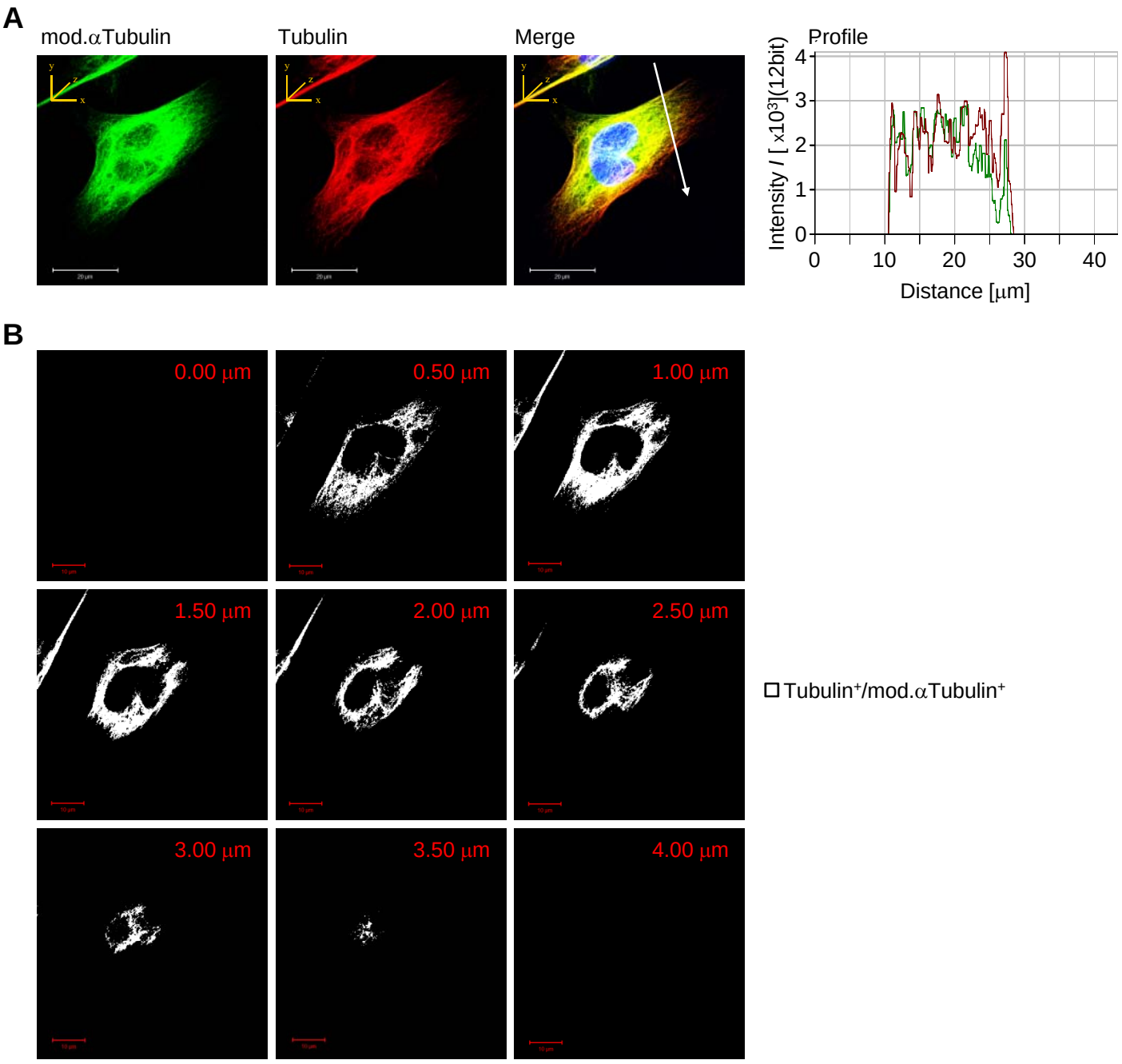

Supplemental Figure 4: 3D-colocalization of the cell-penetrating tubulin antibody and the tubulin⁺ cytoskeleton. (**A**) Representative three dimensional confocal images (left panels) underwent line profiling to demonstrate colocalization of PS-DNA oligo-conjugated cell-penetrating tubulin antibodies (FAM⁺, green) and tubulin⁺ cytoskeleton (red). A2058 tumor cells were cultured with the modified antibodies as in Figure 1A, followed by staining with another tubulin antibody (red) after fixing the cells (right panel). (**B**) Composition of 3D-confocal images shown layer-by-layer including pixel double-positive for modified tubulin antibodies and tubulin⁺ cytoskeleton. Confocal image z-layer stage is indicated. Scale, 20 μm, 10 μm.

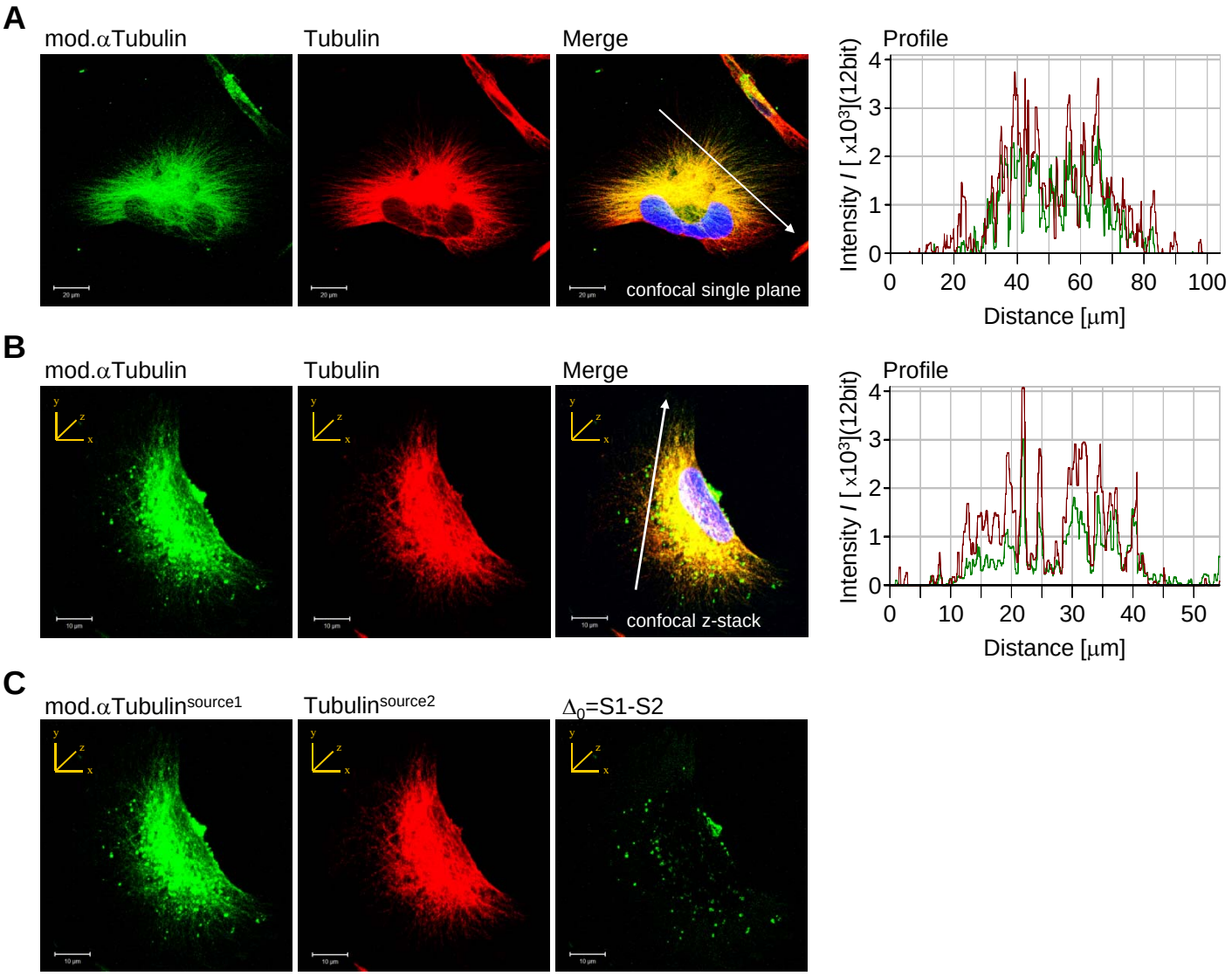

Supplemental Figure 5: 2D versus 3D-colocalization profiling of PS-DNA oligo conjugated tubulin antibodies and tubulin⁺ cytoskeleton including additional signal. (**A**) Two dimensional confocal images (left panels) underwent line profiling to demonstrate colocalization of cell-penetrating modified tubulin antibodies (FAM⁺, green) and tubulin⁺ cytoskeleton (stained by another tubulin antibody after fixing the cells, middle panel). (**B**) Three-dimensional confocal images (left panels) of line profiling demonstrating colocalization of cell-penetrating modified tubulin antibodies (left panel) and tubulin⁺ cytoskeleton (middle panel). (**C**) Potentially occurring additional/residual modified tubulin antibody accumulation visualized following the algorithm D_0=S1-S2, considering modified anti-tubulin emission S1 and tubulin⁺ cytoskeleton emission S2. Scale, 20 μm, 10 μm.

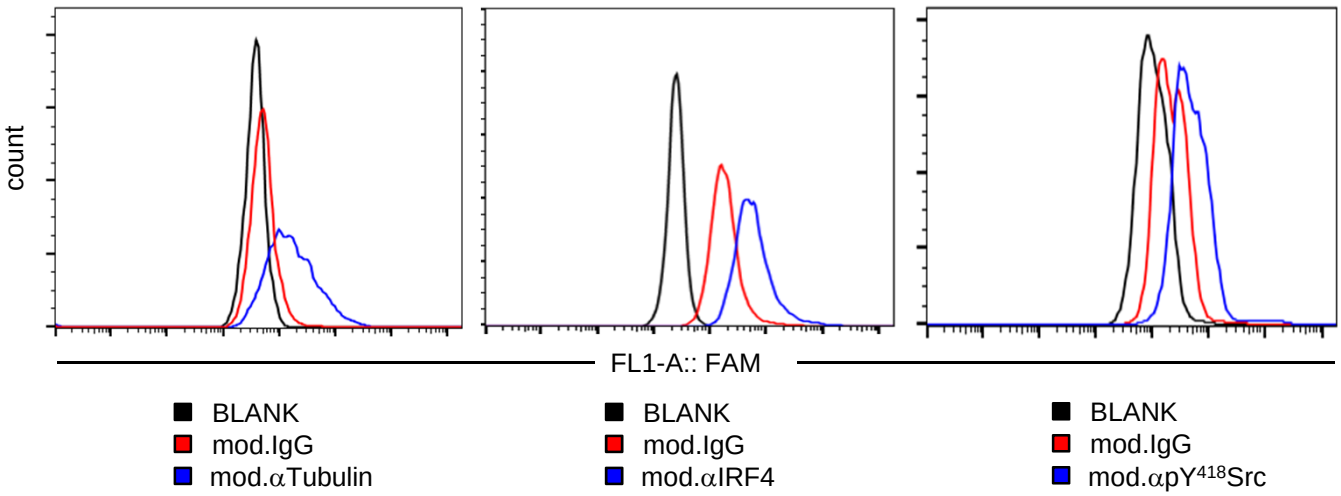

Supplemental Figure 6: PS-DNA oligo-modified non-targeting antibodies do not efficiently accumulate intracellularly. Cellular retention of fluorescently labeled PS-DNA oligo-modified targeting antibodies, anti-tubulin (1 h at 10 μg/ml), anti-IRF4 (7 d at 5 μg/ml) and anti-pY(418)-Src (4 h at 5 μg/ml) was compared to non-targeting modified IgG control antibodies by flowcytometry. Data represent three independent experiments.

A

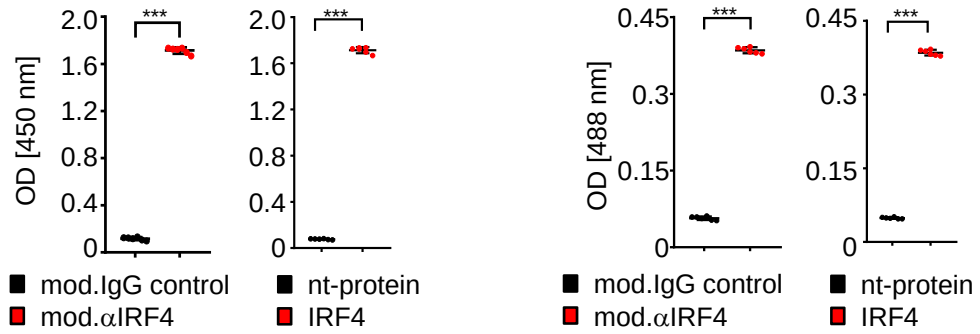
OD [450 nm]
2.0
1.6
1.2
0.8
0.4
0
***
mod.IgG control
mod.αIRF4
nt-protein
IRF4
OD [488 nm]
0.45
0.3
0.15
0

B

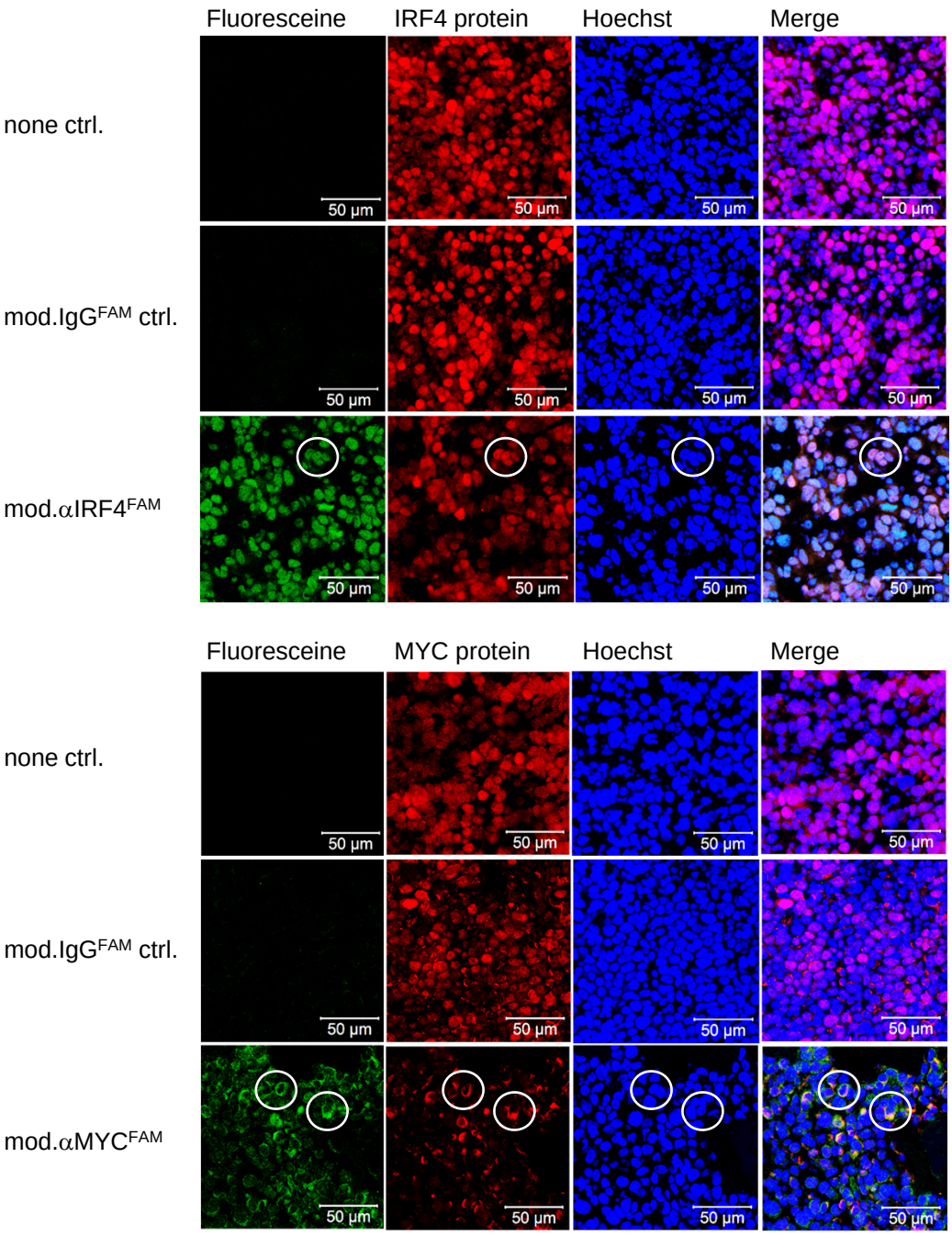
Fluoresceine
IRF4 protein
Hoechst
Merge
none ctrl.
mod.IgG^{FAM} ctrl.
mod.αIRF4^{FAM}
MYC protein
mod.αMYC^{FAM}
50 µm

Supplemental Figure 7: PS-DNA oligo-modified anti-IRF4 and anti-Myc antibodies recognize their targets *in vitro* and/or *in vivo*. (**A**) Antigen (IRF4) recognition by PS-DNA oligo-modified IRF4 antibody was validated by ELISA. ELISA was set up to assess the bound IgG moiety of the modified antibody (OD 450nm, upper panels) and bound FAM moiety of the modified antibody (OD 488 nm, lower panels). Antigen specific recognition was shown by comparing modified IRF4 antibody to modified control IgG (left panels), and by using IRF4 and an irrelevant non-target (nt) protein as antigens (right panels). Representative ELISA data are shown. N=6, SD shown. Unpaired Student's *t* test: ***) $P<0.001$. (**B**) Antigen-targeting fluoresceine-positive PS-modified antibodies (green) colocalize with their targets IRF4 and MYC (red), respectively, in tumor tissues from nice treated with modified anti-IRF-4 or anti-Myc antibodies. Non-targeting fluoresceine-positive PS-modified IgG control antibodies underwent cellular/tissue clearance and were not detectable in tumor tissue microsections. Scale, 50 μm.

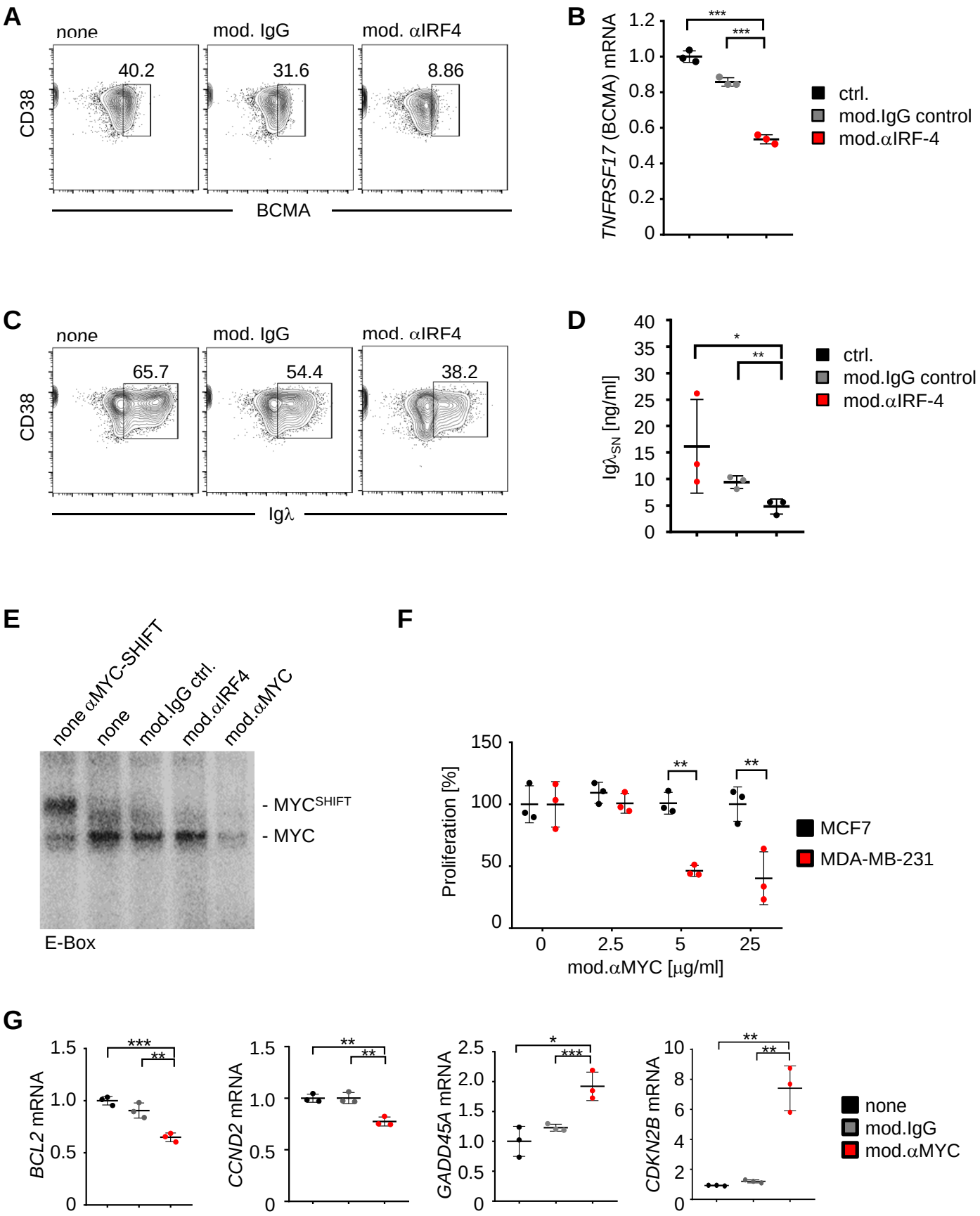
A
none
mod. IgG
mod. αIRF4
40.2
31.6
8.86
CD38
BCMA
B
TNFRSF17 (BCMA) mRNA
ctrl.
mod.IgG control
mod.αIRF-4
C
65.7
54.4
38.2
Igλ
D
Igλ_SN [ng/ml]
E
none αMYC-SHIFT
none
mod.IgG ctrl.
mod.αIRF4
mod.αMYC
- MYC^SHIFT
- MYC
E-Box
F
Proliferation [%]
MCF7
MDA-MB-231
mod.αMYC [µg/ml]
G
BCL2 mRNA
CCND2 mRNA
GADD45A mRNA
CDKN2B mRNA
none
mod.IgG
mod.αMYC

Supplemental Figure 8: Reduced tumor cell survival upon PS-DNA oligo-modified IRF4 antibody or PS-DNA oligo-modified Myc antibody treatment *in vitro*. Human multiple myeloma MM.1S cells were treated with 5 μg/ml of the indicated antibodies for 24 h and expression of tumor cell survival factor BCMA specific for multiple myeloma was assessed by (**A**) flow cytometry at protein level and (**B**) qRT-PCR at mRNA level. Antitumor effect by treating with PS-DNA oligo-modified IRF4 antibody was shown by significantly reduced IgL production by the myeloma cells (**C**) flow cytometry and (**D**) ELISA. All experiments were performed at least 3 times. (**E**) PS-DNA oligo-modified Myc antibody reduces MYC protein binding to target DNA (E-Box) shown by electrophoretic mobility shift assay (EMSA). Nuclear extracts were isolated from human multiple myeloma MM.1S cells treated with 10 μg/ml of the indicated antibodies for 48 hr. Myc protein containing DNA complex was verified by supershift analysis (lane 1). (**F**) Modified Myc antibody significantly decreases cell viability of MYC-dependent human breast cancer cells MDA-MB-231 in a dose-dependent manner. MYC-independent human breast cancer cells MCF7 were included as control. Unpaired Student's *t* test was used to compare the results : **) $P<0.01$. (**G**) Modified Myc antibody significantly suppresses Myc-target gene expression in MM.1S cells *in vitro* as assessed by qRT-PCR. Human multiple myeloma MM.1S cancer cells were treated with 10 μg/ml of the indicated antibodies for 48 h before mRNA was harvested. SD is shown. (B, D and G) Unpaired Student's *t* test was used to compare control or mod.IgG control and mod.αIRF-4 or mod.αMYC treatment: *) $P< 0.05$, **) $P<0.01$, ***) $P<0.001$.

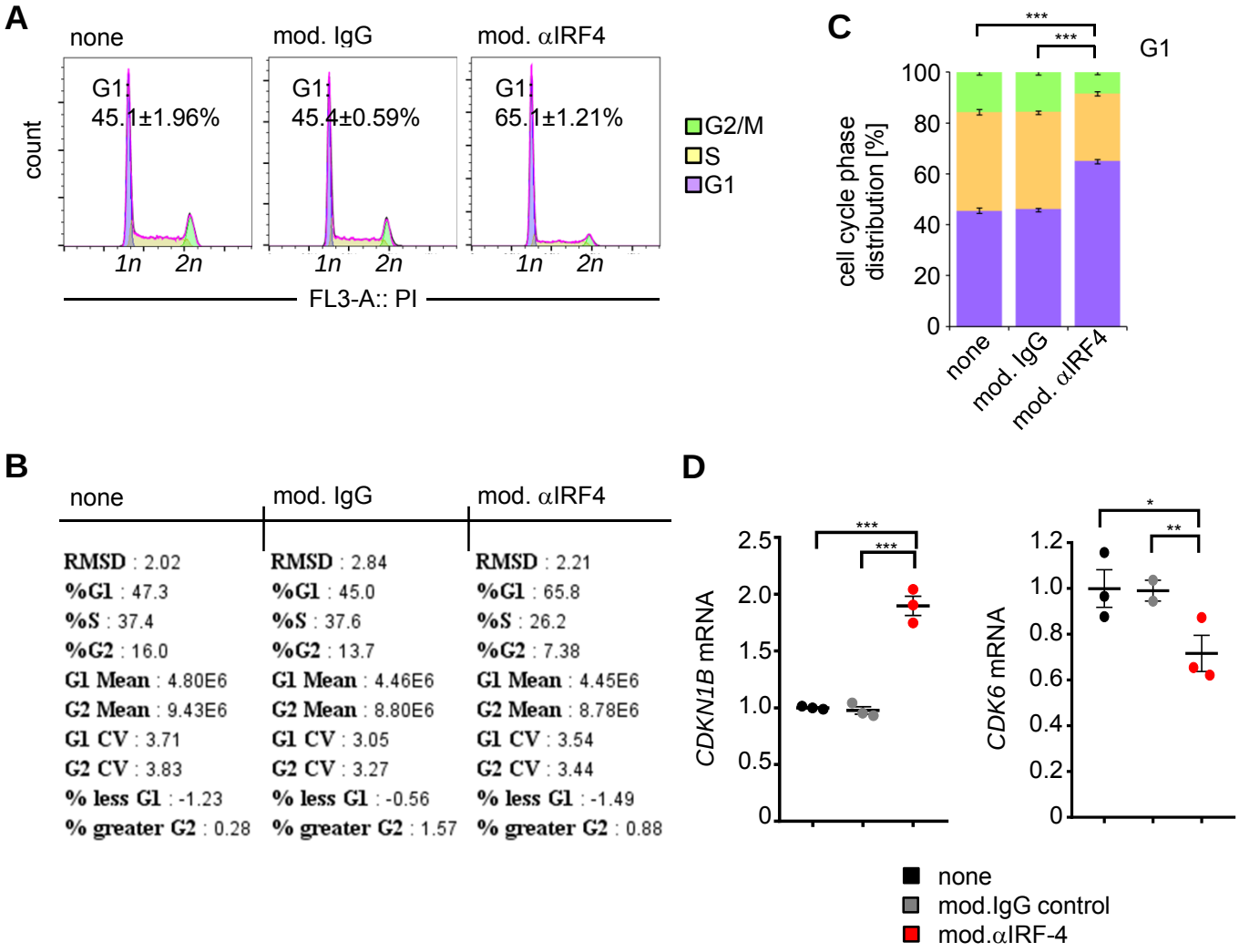

Supplemental Figure 9: Reduced cell-cycle turnover by treating tumor cells with PS-DNA oligo-modified anti-IRF4 antibodies *in vitro*. Human multiple myeloma MM.1S cells were treated daily with 5 μg/ml of the indicated antibodies. (**A**) cell cycle analysis was performed and analyzed by flow cytometry. (**B**) Representative cell cycle distribution upon PS-DNA oligo-modified IgG and IRF4 antibody treatment was assessed by flow cytometry. (**C**) Triplicate cell cycle analyses quantification showing cell cycle distribution upon modified IgG and IRF4 treatment. (**D**) RT-PCR showing expression of cell cycle regulators, human CDKN1B and CDK6 in human multiple myeloma cells MM.1S, upon indicated treatments. SEM shown. Unpaired Student's *t* test was used to compare non or mod. IgG control and mod. αIRF-4 treatment: *) $P< 0.05$, **) $P<0.01$, ***) $P<0.001$.

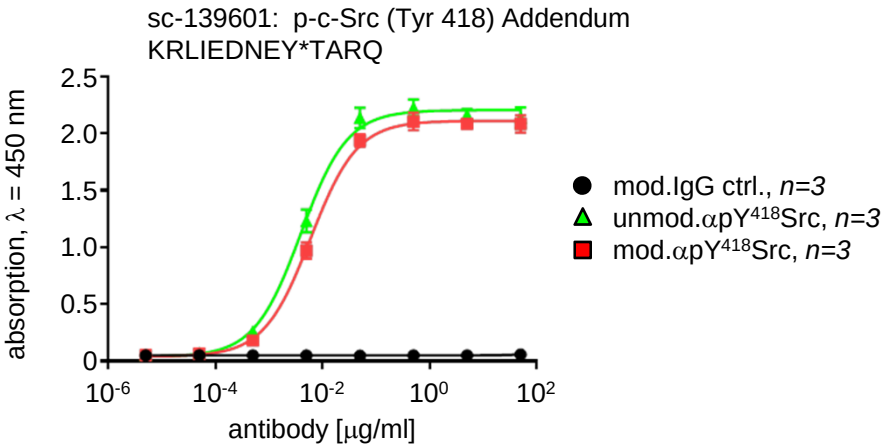

Supplemental Figure 10: PS-DNA oligo-modification of anti-pY(418)-Src antibody does not affect antigen recognition. Antigen (pY(418)-Src) recognition by PS-DNA oligo-modified pY(418)-Src antibody compared to unmodified pY(418)-Src antibody, both titrated as indicated, was not affected by chemical modification as assessed by ELISA (OD 450nm). PS-DNA oligo-modified IgG antibody was employed as non-binding control. Antigen peptide sequence is indicated. The experiment was repeated with similar results.